

GRZEGORZ KAMIŃSKI, RAFAŁ JAKUBOWSKI, EMIL KUPIEC\*

## COOLING METHODS OF LINEAR MOTORS FOR PRT DRIVE

### SPOSOBY CHŁODZENIA SILNIKÓW LINIOWYCH DO NAPĘDU PRT

#### Abstract

This paper presents thermal calculations and tests of a linear induction motor for a model of a personal rapid transit vehicle drive. Various air and liquid cooling systems are analyzed. Laboratory test results of selected solutions are presented. The thermal equivalent circuit model of selected solutions were made. The calculation results were compared with the test results and the most effective solution was selected.

*Keywords: linear induction motor, thermal tests of electrical machines, thermal analysis*

#### Streszczenie

Praca dotyczy obliczeń i badań cieplnych indukcyjnego silnika liniowego przeznaczonego do napędu modelu pojazdu systemu *Personal Rapid Transit*. Przeanalizowano różne układy chłodzenia powietrznego oraz cieczowego. Przeprowadzono badania wybranych rozwiązań układu chłodzenia na rzeczywistym układzie. Wykonano modele matematyczne w postaci sieci cieplnej wybranych rozwiązań. Wyniki badań porównano z wynikami obliczeń oraz wybrano najefektywniejsze rozwiązanie układu chłodzenia rozpatrywanego silnika liniowego.

*Słowa kluczowe: silnik indukcyjny liniowy, badania cieplne maszyn elektrycznych, obliczenia cieplne*

**DOI: 10.4467/2353737XCT.15.057.3857**

\* Prof. D.Sc. Ph.D. Eng. Grzegorz Kamiński, M.Sc. Eng. Rafał Jakubowski, M.Sc. Eng. Emil Kupiec, Institute of Electrical Machines, Faculty of Electrical Engineering, Warsaw University of Technology.

## 1. Introduction

In recent years, constructors' interest in drive implementations using linear motors has increased. Linear motors, due to their ability to convert electrical energy directly to the thrust force of linear motion, are becoming more popular in propulsion systems. In this article, a linear induction motor (LIM) applied as drive for vehicle of personal rapid transit (PRT) system is presented. PRT is an idea of the public transportation system based on small vehicles moving on a special track which perform automated point-to-point transportation of passengers with no stops [1]. A single sided flat linear induction motor with short primary part mounted on vehicle and aluminum reaction plate with back-iron on the track was used as the drive unit [2]. The LIM inductor has open structure and its vulnerable parts, such as end-winding connections, are located nearly to the track structure. Ensuring reliability of operation of this machine in outdoor conditions requires adequate mechanical protection for its parts. Measures used for this purpose should allow for effective heat loss dissipation.

Motor operation in the drive of the PRT vehicle is characterized by a high variability of generated thrust (frequent starts and stops) and variable cooling conditions due to driving speed and high ambient temperature range. Therefore, during the design, it is important to pay particular attention to thermal problems occurring in this type of machine.

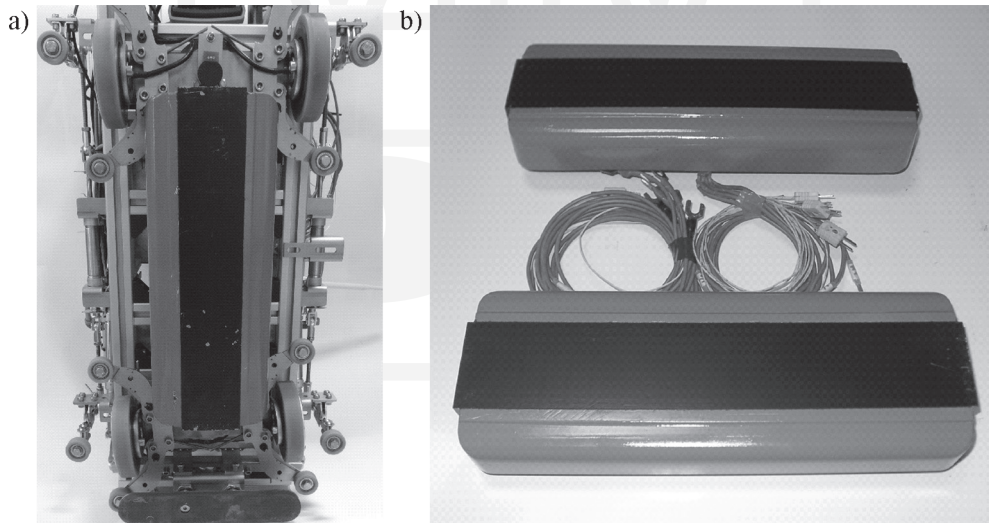


Fig. 1. PRT vehicle model: a) bottom view, b) inductor of the LIM

The article presents a few technical solutions for cooling system for linear induction motors with the short primary part destined for the PRT vehicle model drive.

A model of a PRT vehicle driven by a linear motor is shown in Fig. 1. It consist of an inductor mounted to the vehicle body and bogie, which provides an appropriate air gap between the inductor and the track, keeps the vehicle on the track and supports the change of direction of movement at junctions.

## 2. Cooling methods of linear motors for PRT drive

The following methods of LIM cooling destined for the PRT drive model have been proposed:

- natural convection – the inductor is not equipped with an additional cooling system, heat transfer occurs only through natural convection (Fig. 1a),
- forced convection – fans are installed on the outer surface of the inductor yoke with a vane system directing air flow over the yoke and end-winding connections surfaces (Figs. 2 and 3a),
- free or forced convection – an inductor with a radiator created by the diversity of the dimensions of the inductor yoke steel sheets (Fig. 4a) or by bending the core sheets (Fig. 4b),
- forced convection with liquid cooling medium – inductor with heat exchanger and liquid cooling system.

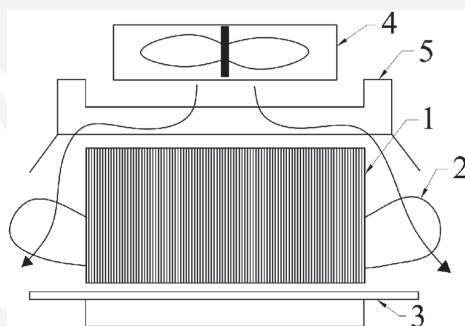


Fig. 2. LIM inductor with convection forced by fans: 1 – core, 2 – end-winding connections, 3 – aluminum reaction plate with back-iron, 4 – fan, 5 – vanes system directing air flow

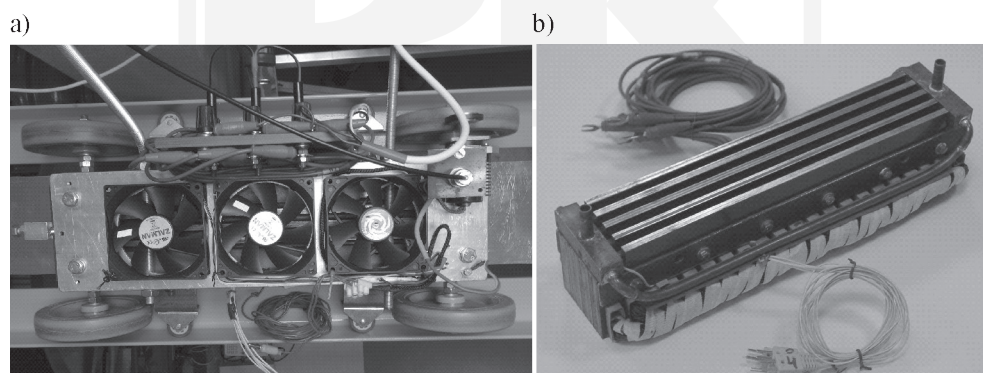


Fig. 3. Model of LIM inductor: a) with convection forced by fans, b) with liquid heat exchanger

An exchanger can be formed by using inductor stack sheets in shapes that ensure the formation of sealed cooling channels and collector channels (Fig. 5) by embedding exchanger pipes into the yoke and end-winding (Fig. 3b) or by using hollow conductors for the inductor winding.

By analyzing the structural terms of the presented cooling methods, it should be noted that the use of LIM solutions with natural cooling creates the necessity of increasing the dimensions of the machine relative to the solutions with forced cooling. An LIM cooling system with a radiator created by differentiated or bended yoke sheets causes an increase in the volume of the motor which in turn causes a larger space in the vehicle reserved for the drive. The solution which provides a compact design of the LIM is a system with a liquid heat exchanger (in the form of pipes with coolant or hollow conductors).

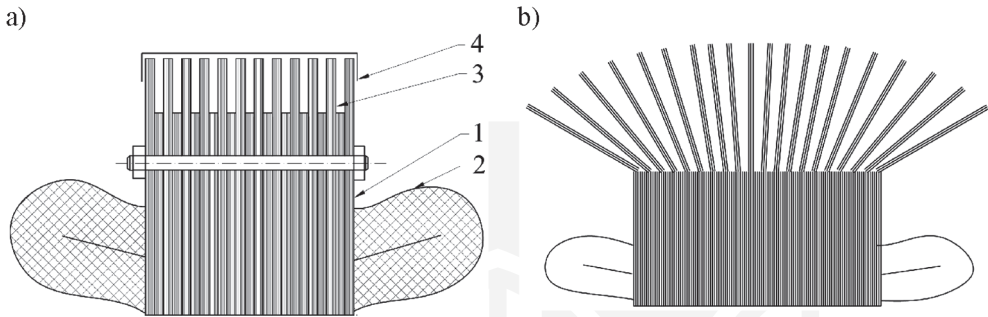


Fig. 4. Inductor with radiator: a) formed by differentiated core sheets, 1 – core, 2 – end-winding connections, 3 – core sheet of various sizes, 4 – cover with vanes system, b) bending core sheet

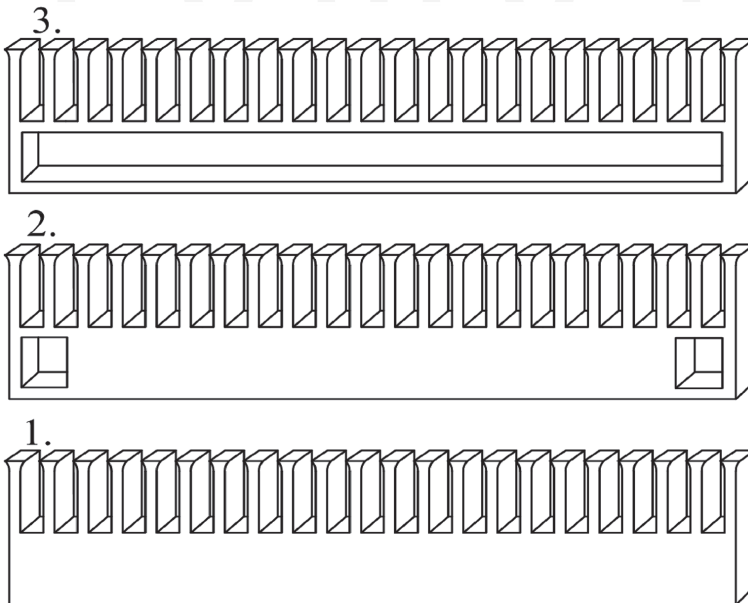


Fig. 5. LIM cooling system with liquid heat exchanger constructed by the use of various steel sheets: 1 – core sheet, 2 – sheets with channels collector, 3 – steel sheets with cooling channel

### 3. Thermal model of linear motor

A parametrical thermal model of an inductor of geometric dimensions shown in Fig. 7 was built. It enables making the calculations for the cooling system with free convection, forced convection and water cooling.

The geometry of the inductor core was simplified to straight teeth without rounded corners of the slots bottom and without teeth shoes – holes for core pressing and mounting bolts were omitted. The geometry of the thermal model is described by the following list of parameters:  $h_{ds}$  – inductor tooth height;  $b_d$  – tooth width;  $b_Q$  – slot width;  $h_j$  – inductor yoke height;  $l_{Fe}$  – length of inductor stack – along the cross-section;  $l_s$  – length of inductor.

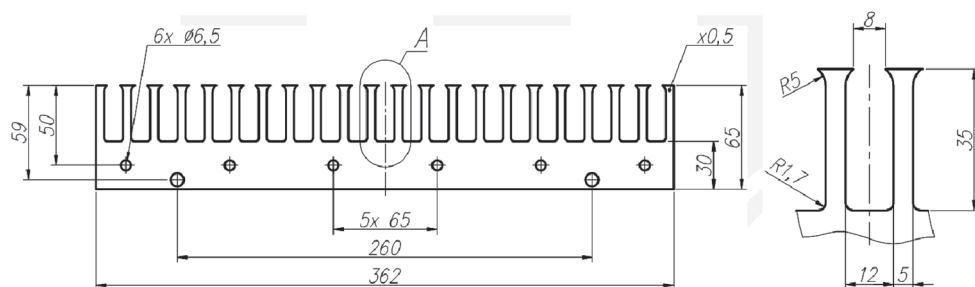


Fig. 7. Dimensions of inductor core model

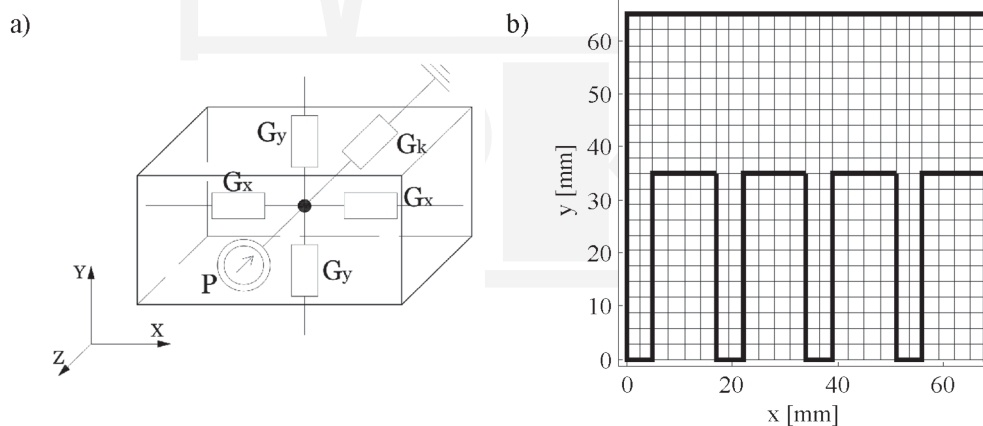


Fig. 8. a) The elementary volume of thermal network and b) fragment of thermal model mesh for the exemplary discretization parameters:  $n_{xQ} = 4$ ,  $n_{xd} = 2$ ,  $n_{yj} = 10$ ,  $n_{ydlQ} = 12$

Due to the symmetry of the LIM along the length of the core and along the width of the stack, the thermal model of the motor represents 1/4 of physical model. The thermal network method was used for modeling steady state temperature distribution in the LIM structure [3–6]. Temperature differences across the width of the stack were neglected, this allowed building a two-dimensional thermal network. The thermal model was divided into elementa-

ry volume by  $ZX$  and  $ZY$  planes of length equal to the width of the stack. The division of the model was described by the following discretization parameters:  $n_{xQ}$  – number of nodes in  $X$ -axis, in area of one slot;  $n_{xd}$  – number of nodes in  $X$ -axis, in area of one tooth;  $n_{yj}$  – number of nodes in the  $Y$ -axis, in area of yoke;  $n_{ydQ}$  – number of nodes in  $Y$ -axis, in teeth and slots area. As a result of discretization, the model was divided into an elementary volume. The fragment of the model with an exemplary discretization is shown in Fig. 8b).

Figure 8a) shows the view of the thermal network model elementary volume described by the following parameters:  $G_x$  – thermal conductance in  $X$ -axis;  $G_y$  – thermal conductance in  $Y$ -axis;  $G_k$  – thermal conductance to the coolant medium;  $P$  – heat source power flowing into volume.

In the presented model, heat transfer to the other elements and to the ambient cooling medium by conduction and convection was taken into account but emission, due to its small contribution to heat transfer, was ignored. Convection occurs in heat transfer from the side and top surface of the inductor yoke to the ambient air or the liquid cooling medium and from the surface of the teeth top and slots to the air gap. In the remaining parts of the LIM, heat transfer occurs by conduction. The power losses in winding and core are here the heat sources. Power losses in the inductor winding were calculated based on winding resistance and the set up currents. Power losses in the yoke and inductor core teeth were determined in the design calculations.

Thermal networks were solved by a method analogous to the nodal potential method used in the electrical networks. Conduction and convection conductance were matched into conductance matrix  $G$ . Power losses and heat fluxes are matched in sources vector  $P$ . The system of equations with unknown temperatures  $\vartheta$ , has the following form:

$$G \cdot \vartheta = P \quad (1)$$

A description of the formulation and solution thermal network algorithm is presented in [4, 5].

#### 4. Thermal tests of linear motor model

Thermal tests of the linear induction motor for the PRT driver were performed for three constructions of the inductor:

- inductor 1 – inductor with impregnated winding,
- inductor 2 – inductor with winding impregnated with resin – monolithic inductor (Fig. 1b),
- inductor 3 – monolithic inductor with liquid heat exchanger (Fig. 3b).

The tested physical models of the inductor were equipped with temperature sensors at the following points:  $T_1$  – bottom of the slot;  $T_2$  – between layers of winding;  $T_3$  – under winding wedge;  $T_4$  – in end-winding;  $T_5$  – between heat exchanger pipe and stack;  $T_w$  – temperature of water in exchanger. Sensors  $T_5$  and  $T_w$  were only used in the inductor with a liquid heat exchanger. Heating tests were performed for three inductor constructions at various cooling conditions:

- inductor 1 with natural cooling,
- inductor 1 with forced convection,
- inductor 2 with natural cooling,
- inductor 2 with forced convection,
- inductor 3 with liquid cooling system,
- inductor 3 with liquid cooling system without radiator fan.

100°C was set as the temperature limit for the LIM model. A series of heating tests for different values of the stator current were performed until a steady state or temperature limit had been reached. Heating test of inductor 3 for inductor winding current  $I = 6$  A and working cooling system is shown in Fig. 9.

In Figure 10, heating curves of inductor physical models for presented cooling conditions were compared.

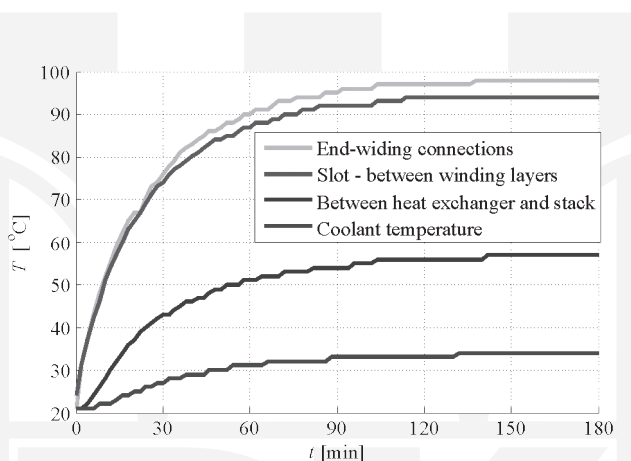


Fig. 9. Temperature vs. time of monolithic inductor supply current  $I = 6$  A with working cooling system

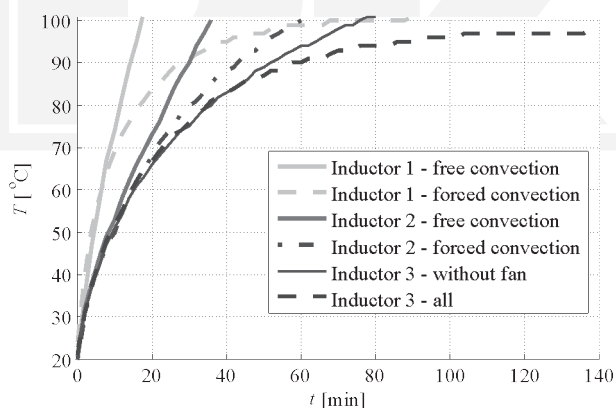


Fig. 10. Comparison of heating curves presented version of LIM supplied with current  $I = 6$  A

Through the use of the liquid cooling system, there was a possibility to achieve more than a double increase in inductor heat transfer capacity from inductor elements (from 122 W to 300 W), owing to this, the continuous current for this version of the inductor is  $I = 6$  A. The same

power losses ( $\sim 300$  W) can dissipate air forced convection cooling system of inductor 1. In the case of failure of the radiator fan of inductor 3, power losses possible to dissipate decreases to 236 W. Inductor 3 has a higher time constant in comparison to inductor 1. When analyzing heating curves, it should be noted that the increase in power losses in the LIM inductor during its heating, may result in deforming the heating curve from the exponential curve.

## 5. Thermal calculations of the linear motor model

A series of thermal calculation models with free, forced, and water cooling were performed. In Figure 11, the distribution of average temperature along the length of the inductor core on specific core heights for inductor 3 with working cooling system and supplied current  $I = 6$  A is shown.

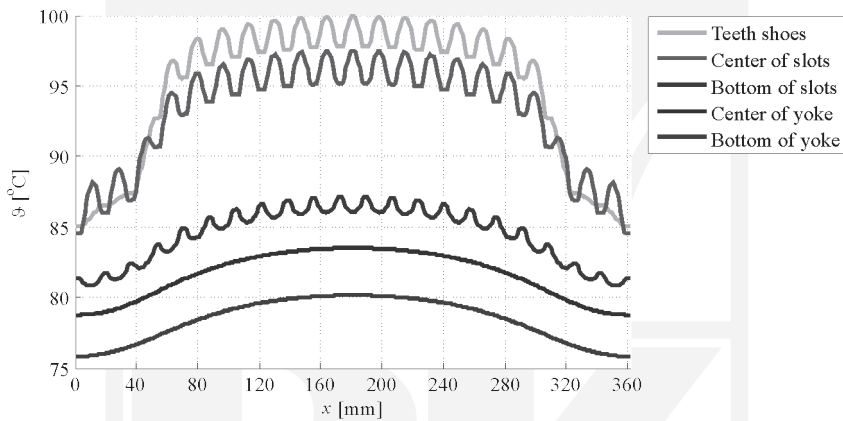


Fig. 11. Temperature distribution in the longitudinal section of the LIM model for current  $I = 6$  A and forced water cooling

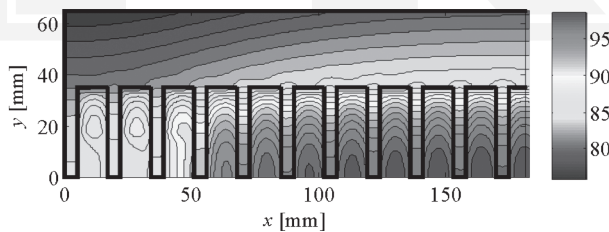


Fig. 12. Temperature map of half of longitudinal section of LIM model for current  $I = 6$  A and forced water cooling

Figure 12 shows the temperature map at half of the longitudinal section of the inductor.

The local temperature increases correspond to inductor slots that generate the most losses. Lower temperature of core edges result from the winding scheme of the machine. In three peripheral slots at the end of inductor stack, there was only one layer of winding – due to this,

these regions had generated half of the heat losses. The highest temperature value occurs in the central axis of the slot. The temperature between the layers of winding in the middle slot of inductor 3 cooled by water is  $98^{\circ}\text{C}$  and this is close to the result obtained from measurements.

In order to establish the relationship between the maximum temperature of the inductor winding and the supply current for air and water cooling methods, a series of calculations of the LIM thermal network model were made. Calculation results are shown in Fig. 13.

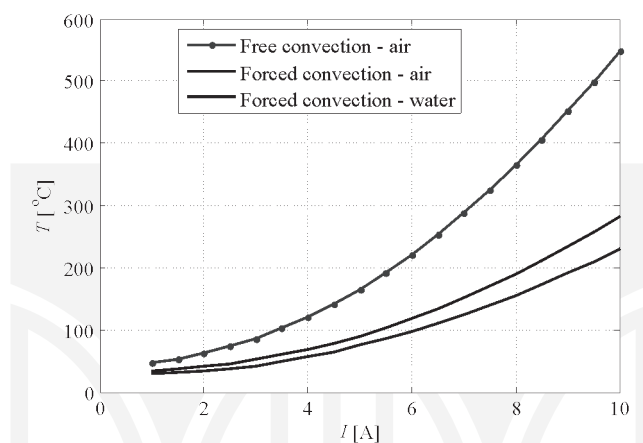


Fig. 13. Dependence maximum temperature in LIM model on inductor current for three cooling methods

The current increase causes a disproportional increase in maximum temperature. Increasing cooling intensity decreases the temperature value.

## 6. Summary

The paper presents selected methods of cooling LIM designed for the model of the PRT vehicle driver. Results of research and calculations of the physical model of LIM were presented.

The calculation results correspond to a large extent with the results of research. The occurring differences between measured and calculated values of temperature are caused by simplified assumptions in the mathematical model and the difficulty in obtaining proper thermal conductivity data and convection coefficient, which is strongly dependent on the temperature and the characteristic dimensions of heat sink surface.

The use of active cooling methods of the inductor allows more than a double increase in value of drained power losses from its inside and thus a corresponding increase in rated thrust force. It should be noted that in the water cooling system, there occurs the relatively large temperature difference between the winding (primary source of heat) and the heat exchanger, which means high resistance in this part of the thermal circuit. Reducing value of this thermal resistance by transferring heat exchanger on the bottom of the slots or making the winding of the hollow conductor makes it possible to further improve the efficiency of the drain heat losses from the inductor.

## References

- [1] Fitcher D., *Individualized automatic transit and the city*, Chicago, Illinois 1964.
- [2] Kamiński G., Herbst A., *Porównanie wyników elektromagnetycznych obliczeń polowych 2D i 3D dla jednostronnego indukcyjnego silnika liniowego*, Zeszyty Problemowe – Maszyny Elektryczne, 2011, nr 93, pp. 109–112.
- [3] Szczypior J., Jakubowski R., *Układ chłodzenia i obliczenia cieplne maszyny z magnesami trwałymi i zewnętrznym wirnikiem*, Zeszyty Problemowe – Maszyny Elektryczne, 2014, nr 103, pp. 151–156.
- [4] Krok R., *Sieci cieplne w modelowaniu pola temperatury w maszynach elektrycznych prądu przemiennego*, Monografia, Wydawnictwo Politechniki Śląskiej, Gliwice 2010.
- [5] Szczypior J., Jakubowski R., *Obliczenia cieplne w bezrdzeniowej maszynie dyskowej z magnesami trwałymi o chłodzeniu bezpośrednim*, Zeszyty Problemowe – Maszyny Elektryczne, 2009, nr 83, pp. 59–66.
- [6] Szczypior J., Jakubowski R., *Metody bezpośredniego chłodzenia uzwojenia w bezrdzeniowej maszynie dyskowej z magnesami trwałymi*, Zeszyty Problemowe – Maszyny Elektryczne, 2010, nr 88, pp. 109–115.

